



Effects of Photobiomodulation Using Low-Power Diode Laser Therapy and Nano-bone on Mandibular Bone Regeneration in Rats

Latifa Mohamed Abdelgawad^{*}, Kawashty Ali Mohamed, Ahmed Abbas Zaky

Medical Applications of Lasers Department, National Institute of Laser Enhanced Science (NILES), Cairo University, Giza, Egypt

***Correspondence to**
Latifa Mohamed Abdelgawad,
Emails: latifa.mohamed@cu.edu.eg
and latifa@niles.edu.eg

Received: December 24, 2023
Accepted: May 18, 2024
Published: October 8, 2024



Abstract

Introduction: Recently, the positive effects of photobiomodulation (PBM) and nano-bone on bone regeneration have garnered significant attention. The purpose of the research was to assess the impact of PBM and nano-bone on the process of mandibular bone repair in mice.

Methods: A 4-mm diameter bone defect was created in the left mandibular angle of 24 mice separated into 4 equal groups: group I: control; group II: PBM by irradiation at 100 mW of a 980 nm diode laser for one minute (three sessions per week; day on and day off); group III: nano-bone; group IV: PBM with nano-bone. Every group was sectioned into 3 equal subgroups corresponding to the evaluation method period: (A) one week, (B) two weeks, and (C) four weeks. Histological examination was done with hematoxylin, eosin, and Masson's Trichrome after one, two and four weeks for inflammation, bone defect coverage, vascularization within the newly formed bone, and new bone formation. Statistical analysis of the data was done and presented as percentage values using chi-square. The significance level was set at P value ≤ 0.05 within all tests.

Results: In general, by histological examination of the mandibular bone defect of the rats, the intensity of inflammation was the least in group IV when compared with groups II and III and the control group at all evaluation periods ($P < 0.001$). Also, group IV showed a high significant rise in the percentage of new bone formation following four weeks when compared with the control ($P \leq 0.001$) and groups II and III ($P < 0.001$).

Conclusion: The present research results confirmed that the combination of PBM and nano-bone can aid in the repair of mandibular bone abnormalities. This animal study suggests that the use of PBM and nano-bone should be investigated further in clinical studies.

Keywords: Photobiomodulation; Nano-bone; Bone regeneration; Rats.

Introduction

The repair of bone defects is an important health issue not yet completely resolved. Thus, novel potential therapeutic methods are urgently needed. So, the application of photobiomodulation (PBM), as well as nanomaterials can solve different problems in bone healing.¹⁻⁴

Photobiomodulation therapy (PBMT) utilizes low-power laser light, light emitting diodes, or non-coherent light to activate natural chromophores (such as cytochrome C oxidase & intracellular water) within cells. This stimulation triggers photophysical and photochemical processes at different biological levels, resulting in medicinal effects.⁵⁻⁷

Continuous mode near-infrared (NIR) lasers are the most prevalent type of PBM. Biostimulatory impacts are contingent upon various parameters, with the dose and wavelength being the most significant. It has been proposed that by employing PBM at an appropriate dose and within the near-infrared spectrum, it is possible to

improve the efficacy of promoting bone remodeling and healing. Consequently, PBM has emerged as a promising alternative therapy in the field of bone regeneration. Nevertheless, various investigations utilize distinct parameters of PBM, and cumulative information on the utilization of PBM to enhance bone formation in clinical investigations is limited.⁸⁻¹³

Bone promotes vascularization, osteoblast activity, cell proliferation, and collagen deposition, according to several prior studies. LLLT promotes the formation of new bone and enhances the expression of osteogenic genes in the early phases of bone repair.^{5,14-18}

The domain of nanotechnology has witnessed significant advances in recent years, particularly with regard to the utilization of nanomaterials in regenerative medicine. Numerous published studies have provided evidence of the application of nanomaterials in the process of bone regeneration.¹⁹⁻²⁰

Additionally, nano-bone, which is composed of granules

smaller than one hundred nanometers, is available for purchase. The nanostructure of bone exhibits a higher degree of similarity to that of natural hydroxyapatite. The favorable biological impacts of nano-bone are due to its larger surface area, surface roughness, and wettability include enhanced protein adsorption, improved adhesion of the osteoblasts and mesenchymal stem cells (MSCs), differentiation and proliferation, and enhanced osteoclast response.²¹⁻²³

Important criteria for successful bone regeneration include the osteoinductivity, biocompatibility, and mechanical properties of nano-bone. Furthermore, the response to bone formation can be altered by modifying the mechanical environment. Furthermore, the efficacy of biomaterials in promoting bone healing is significantly influenced by their biocompatibility. Among these properties, osteoinductivity stands out as the most critical, as it is responsible for stimulating the formation of new bone.²³⁻²⁶

Several investigations have been undertaken on the application of nano-bone for bone regeneration. Although several studies have examined the potential of PBMT (utilizing various types and low-power lasers) to improve bone regeneration, there is a scarcity of data regarding the combined application of PBMT and nano-bone in this regard. The purpose of this investigation was to assess the impact of PBM and nano-bone on the rate of mandibular bone regeneration.

Null hypothesis: Neither PBM nor nano-bone has an influence on the regeneration of a rat's mandibular bone.

Material and Methods

Selection of the Animals

Animals used in this study were 24 male Wistar rats aged 9 to 12 weeks, with a weight range of 240-260 g. The rats were housed in suitable cages, with six animals per cage. Each mouse was individually identified by a marking on its tail. The rats were maintained under a twelve-hour light-dark cycle and had unrestricted access to water and food.²⁷

Anesthesia of Rats

Rats were anesthetized by using ketamine chloride (Clorketamin 1000; Vetoquinol, Fort Worth, TX) 5 mg/kg intramuscularly with the injection of xylazine chloride (Eurovet Animal Health B.V., Bladel, The Netherlands) three milligrams per kilogram to obtain muscular relaxation, and then local injections of a solution containing epinephrine and half percent lidocaine were administered to anaesthetize the gingival tissues of the mandible. This was done to reduce pain and bleeding throughout the procedure.²⁷

Surgical Procedure

Unilateral mandibular defects were created in all twenty-

four anesthetized rats as labelled previously.²⁸ In brief, bone defects were made near the angle of the left side of the mandible with a 4-mm circular drill in a low-speed handpiece under constant sterile saline coolant after a full thickness flap reflected to expose the mandible under general anesthesia. Finally, the soft tissue was repositioned, and the incision was closed with sutures made of five to zero nylon thread (Figure 1).

Rats were given buprenorphine (using a formula depending on their weight) every twelve hours over a period of three days to manage pain after surgery. Additionally, the mice were fed a soft food diet for one week following the operation.²⁸

Laser Irradiation Technique

The laser irradiation of mandibular rat bone defects in group II and group IV was carried out with a continuous-wave 980-nm diode laser (Den Lase. China) at output power of 100 mW for 60 seconds (30 seconds labial and 30 seconds Lingual) three times (day on and day off) for PBM with a standard handpiece (Gaussian beam) in non-contact mode 2-mm away from the bone defect^{5,10} (Figure 2 and Table 1).

Application of Nano-bone Material

According to the manufacturer's instructions, Nano-Bone ((Dentaurum, Germany) was applied locally to a bone defect after being mixed with saline until a sticky paste consistency (Figure 3).

Experiment Design

The Twenty-four rats with mandibular bone defects were randomized by simple random sampling and separated into 4 equal groups: group I: control; group II: PBM by irradiation at 100 mw of a 980 nm diode laser for one minute; group III: nano-bone; group IV: PBM with nano-bone.

Histological Analysis

Rat mandibular specimens were obtained at one, two, and four weeks post-surgery and preserved in a four percent paraformaldehyde phosphate buffer (Fujifilm Wako Chemical, Osaka, Japan). The collected samples were decalcified by soaking them in a solution containing ten percent of ethylenediaminetetraacetic acid for a period of fourteen days at normal room temperature. Subsequently, the samples were dehydrated by using a series of ethanol solutions and finally embedded in paraffin. The sections were produced with a three-micrometer thickness in the anteroposterior plane. To conduct a descriptive study, we applied hematoxylin and eosin to each section. In addition, Masson's trichrome staining was utilized for histochemical investigation. This staining method revealed the newly formed collagen and osteoid by a blue or green reaction, while the cytoplasm of the cells was

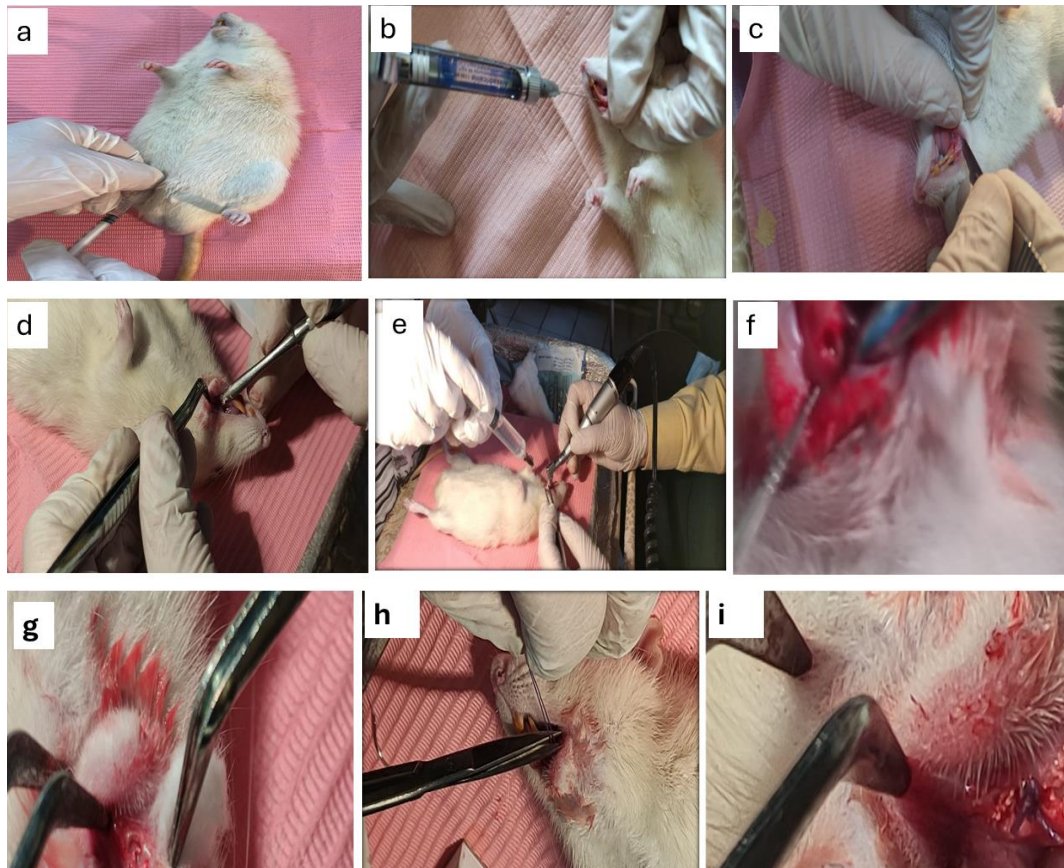


Figure 1. Surgical Steps for Induction of Bone Defect in the Rat Mandibula. (a) Rat anaesthesia, (b) local anaesthesia in the surgical site, (c) surgical incision, (d) retraction of the flap, (e) drilling of bone defect, (f) bone defect (g) cleaning the surgical field, (h) suturing the surgical site, (i) surgical site after suturing

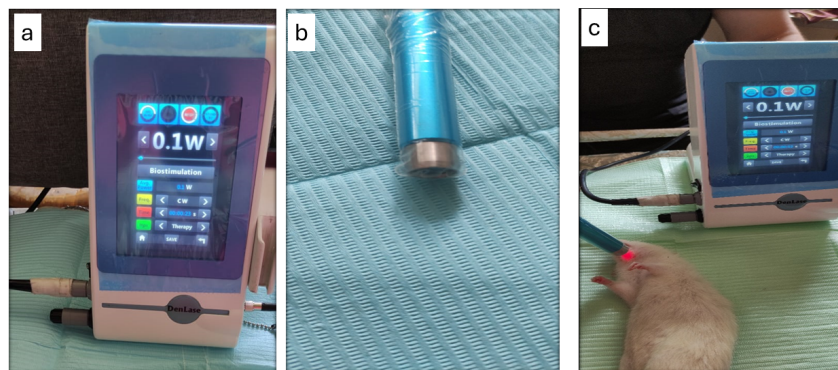


Figure 2. Laser Irradiation Technique for Mandibular Rat Bone Defects. (a) 980 nm diode laser (Denlase), (b) laser biostimulation tip, (c) laser irradiation of bone defect

Table 1. Laser Parameters used in This Study

| Parameters | Diode Laser |
|--------------------------|---|
| Wavelength | 980 nm (Den Lase. China) |
| Mode | Continuous wave |
| Power | 100 mw |
| Tip | Biostimulation tip |
| Position | 2 mm from the tooth surface |
| Exposure time | 30 seconds for two times with a total exposure time of one minute |
| Number of laser sessions | three times (day one and day off) |

indicated by a red reaction.²⁷⁻³⁰

Statistical Analysis

We used the frequencies and percentages of categorical data in the chi-square test for analysis. In each of the experiments, the level of significance was established at $P \leq 0.05$. We conducted the statistical analysis using Version 20 of IBM® SPSS® Statistics for Windows.

Criteria for Histological Evaluation

The histology slides were examined by a pathologist in a blind manner, meaning they were ignorant of the precise

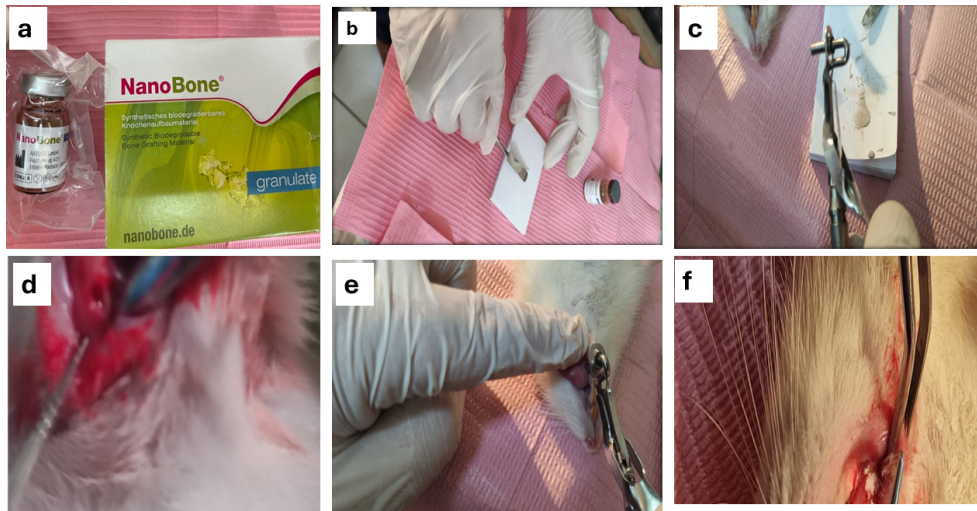


Figure 3. Technique of Nano-Bone Application. (a) nano-bone granules, (b) mixing of nano-bone, (c) loading the nano-bone with a carrier, (d) dryness of bone defect, (e) application of nano-bone to bone defect, (f) bone defect with nano-bone after application

bone regeneration procedure or time interval associated with each slide. The pathologist assessed the severity of inflammation and the amount of bone apposition. The slides were evaluated based on the criteria and scoring system outlined in [Table 2](#).

Results

Group I: Control (After One, 2, and 4 Weeks)

After one week of the surgical bone defect, there was a high quantity of chronic inflammatory cell infiltration and fibroblastic activity with newly formed capillaries. No bone formation could be noticed ([Figures 4A1, 5A1 and 6A](#)). After 2 weeks, microscopic examination still showed moderate chronic inflammatory cell infiltration and fibroblastic activity. Besides, small focal areas of osteoid tissue started to develop ([Figures 7A1, 8A1 and 6B](#)). After 4 weeks, thin newly formed bone trabeculae encircling the surgical bone defect margins surrounded by osteoid tissue and fibro cellular tissue were detected. The thickness of the formed bone was found to be less than that formed in all other study groups ([Figures 9A1, 10A1 and 6C](#)).

These data demonstrated a statistically significant variation between both evaluation intervals (2 and 4 weeks) when compared with one week ($P \leq 0.001$) ([Table 3](#)).

Group II: Photobiomodulation (After One, 2, and 4 Weeks)

Histological examination after one week showed moderate chronic inflammatory cell infiltration, marked vascularity and fibro cellular condensation within and around the bone defect as well as at the periphery of the bone defect forming a capsule. Osteoblasts and osteoclasts were observed at the periphery of the bone defect ([Figures 4 A2, 5 A2 and 6A](#)). Histological findings after 2 weeks showed that there was still a small amount of chronic inflammatory cells and osteoblasts and osteoclasts at the

periphery of the bone defect ([Figures 7B2, 8B2 and 6B2](#)). After 4 weeks, osteoid tissue was still present, and newly formed bone with uneven thickness was detected in the bone defect ([Figures 9 C2, 10 C2 and 6C](#)).

These data displayed statistically significant distinctions between both evaluation periods (one and 2 weeks) ($P \leq 0.5$), and a statistically significant difference between both evaluation periods (one and 4 weeks; $P \leq 0.001$) ([Table 3](#)).

Group III: Nano-bone (After One, 2, and 4 Weeks)

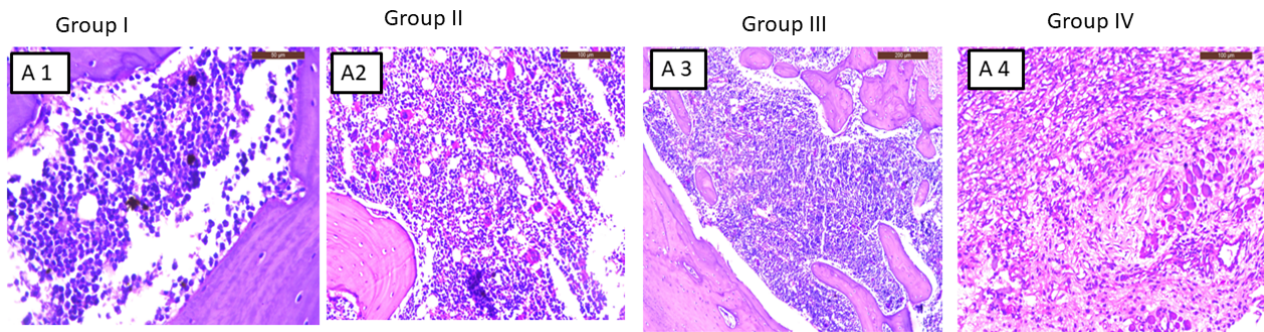
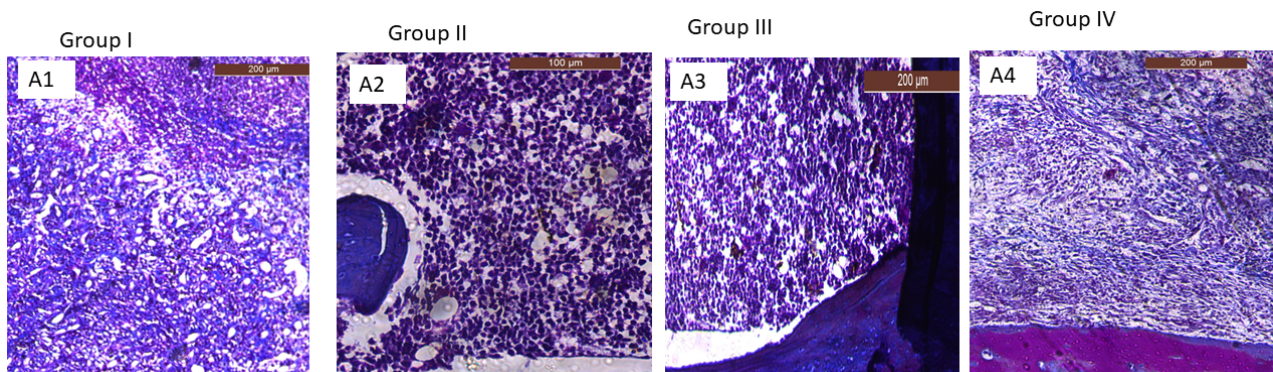
Histological findings after one week showed fewer chronic inflammatory cells in comparison to the control groups at the same evaluation period with marked vascularity and fibroblastic activity surrounding the nano-bone material. Active osteoblasts were observed ([Figures 4 A3, 5 A3 and 6A](#)).

After 2 weeks, a microscopic examination revealed that marked vascularity and a small amount of chronic inflammatory cell infiltration were still present. There is a large quantity of well-organized newly formed trabecular bone with basophilic reversal lines. Osteoid tissues encircled with active osteoblasts were also detected. A thin area of newly formed bone was also detected ([Figures 7 B3, 8B3 and 6B](#)). After 4 weeks, histological examination of the bone defect showed more quantities of well-organized newly formed bone trabecula. These bone trabeculae appeared thicker and more organized lamellar bone than those of the control groups at four weeks ([Figures 9C3, 10C3 and 6C](#)).

The amount of new bone formation illustrated a great percentage histologically at 2 weeks. This percentage continued to increase to reach the maximum level in this group at 4 weeks. There was a statistically significant distinction between the two evaluation times, as indicated by this information (2 and 4 weeks), when compared with one week ($P \leq 0.001$) ([Table 3](#)).

Table 2. The Scoring System Used for Bone Healing

| Score | Bone Defect Coverage Percentage of Defect Bridged by Bone | New Bone Type Nature of New Bone Within the Defect | Vascularization Presence of Vascularization Within the Newly Formed Bone | Inflammation Presence of Inflammatory Cells Around the Newly Formed Bone |
|-------|---|--|---|---|
| 0 | 0% | No new bone | No evidence of neovascularization | Abundant inflammation and Evidence of encapsulation |
| 1 | 1-24 % | Predominantly Woven | few new vessels < 10 (number of new blood vessels less than 10 blood vessel). | Relatively few inflammatory cells ranged from 10-50 (number of inflammatory cells ranged between 10 and 50 cells) |
| 2 | 25-49% | Predominantly lamella remodelled | Abundant neovascularization | No evidence of inflammatory cell presence |
| 3 | 50-74 % | | | |
| 4 | 75-100 % | | | |

**Figure 4.** Photomicrographs of Hematoxylin and Eosin Histological Stained Sections of Bone Defect After One Week in Different Groups of Treatment With a Scale of 200 μm . A1: control group, A2: PBM group, A3: Nano-bone group, and A4: combined group of nano-bone and PBM; high inflammatory cell infiltration with no bone formation is shown after one week**Figure 5.** Representative Microscopic Images of Masson's Trichrome Stained Tissue Sections of Specimens Bone Defect After One Week in Different Groups of Treatment With a Scale of 200 μm . A1: control group, A2: PBM group, A3: Nano-bone group, and A4: combined group of nano-bone and PBM; high inflammatory cell infiltration with no bone formation is shown after one week

Group IV: Nano-bone and PBM (After One, Two, and Four Weeks)

Histological examination after one week showed marked fibrous tissue proliferation near the bone defect with mild to moderate chronic inflammatory cell infiltration and marked vascularity. Few Osteoid tissue formations could be detected away from the surgical bone margins. The graft material was seen in the bone defect (Figures 4A4, 5A4 and 6A). After 2 weeks, connective tissue proliferation in the form of collagen fibers, osteoid tissue, osteoclasts, and osteoblasts were observed in and around the bone defect. New bone formation near the surgical bone margins progressed toward the

center of the bone defect that has the smallest thickness of new bone (Figures 7B4, 8B4 and 6B). Microscopic findings after 4 weeks exhibited marked well-developed lamellar bone trabeculae with basophilic reversal lines (Figures 9C4, 10C4 and 6C).

It was noted that throughout all assessment periods, group IV exhibited a significantly greater percentage of newly formed bone in comparison to the control group ($P \leq 0.001$). Additionally, group IV demonstrated an extremely significant distinction in comparison to groups II and III at all assessment periods ($P < 0.001$). In conclusion, significant differences were observed between groups II, III, and IV and the control group ($P < 0.05$) (Table 3).

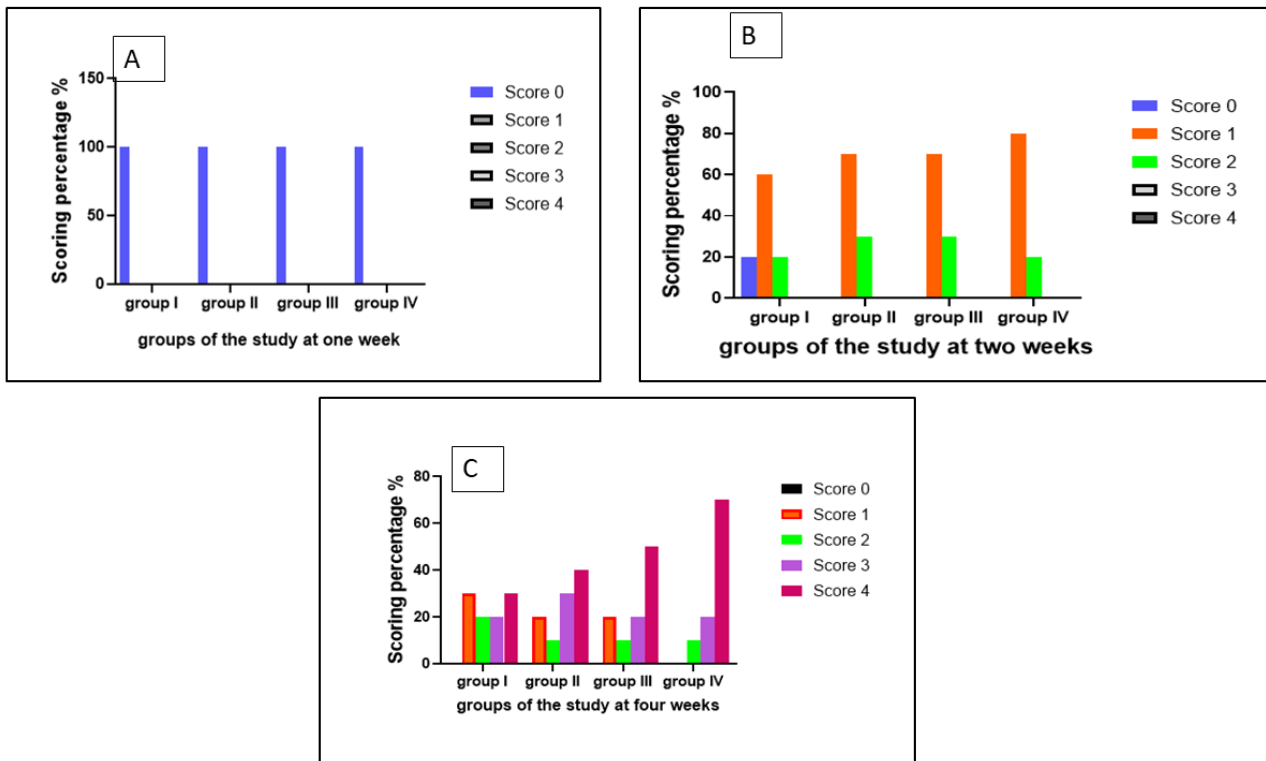


Figure 6. Scoring Percentage of Bone Regeneration in Different Study Groups: One Week (A), Two Weeks (B) and Four Weeks (C)

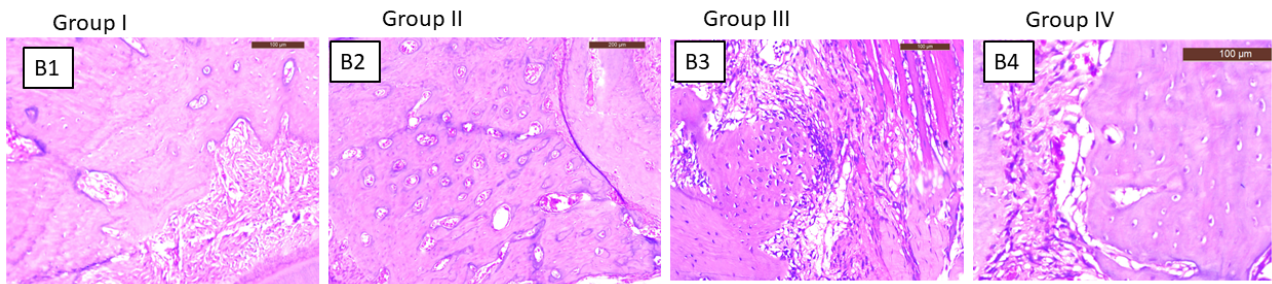


Figure 7. Photomicrographs of Hematoxylin and Eosin Histological Stained Sections of Bone Defect After Two Weeks in Different Groups of Treatment With a Scale of 200 µm. B1: control group, B2: PBM group, B3: Nano-bone group, and B4: combined group of nano-bone and PBM; less inflammatory cell infiltration with new bone formation is shown after two weeks

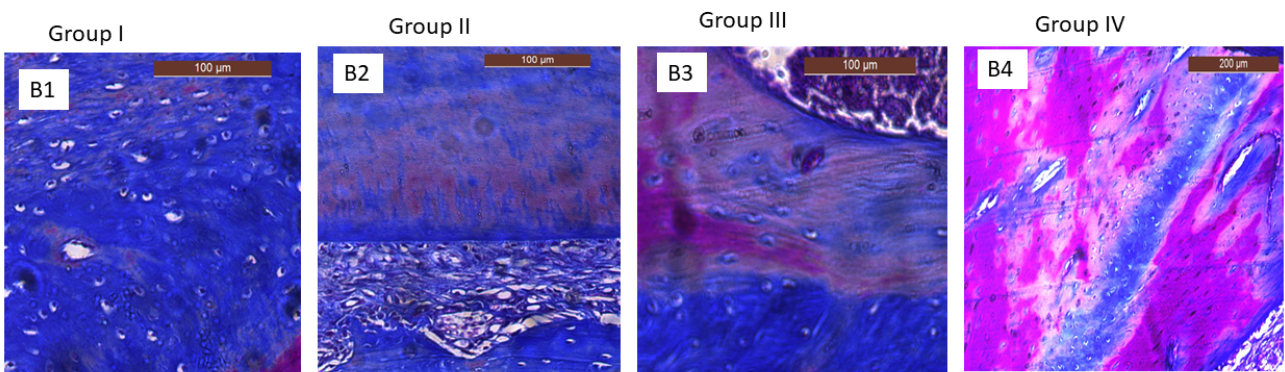


Figure 8. Histological Photomicrographs of Specimens Bone Defect With Masson's Trichrome After Two Weeks in Different Groups of Treatment With a Scale of 200 µm. B1: control group, B2: PBM group, B3: Nano-bone group, and B4: combined group of nano-bone and PBM; less inflammatory cell infiltration with new bone formation is shown after two weeks

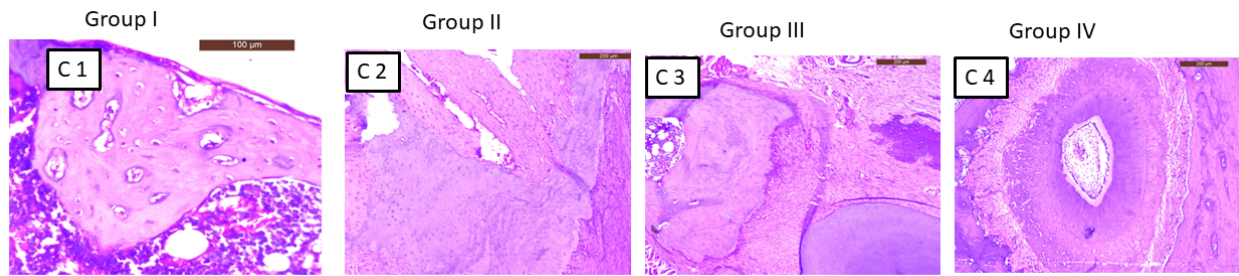


Figure 9. Photomicrographs of Hematoxylin and Eosin Histological Stained Sections of Bone Defect After Four Weeks in Different Groups of Treatment With a Scale of 200 µm. C1: control group, C2: PBM group, C3: Nano-bone group, and C4: combined group of nano-bone and PBM; woven bone formation is shown after four weeks

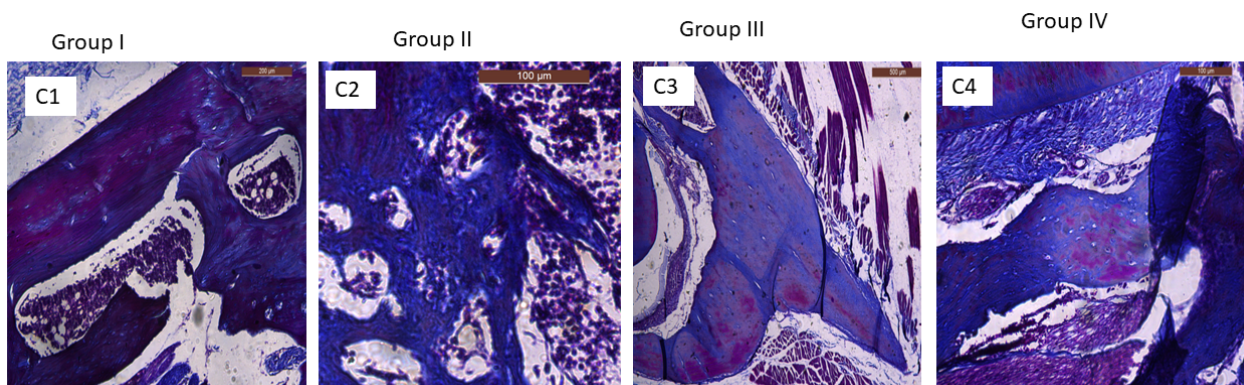


Figure 10. Histological photomicrographs of Specimens Bone Defect With Masson's Trichrome After Four Weeks in Different Groups of Treatment With a Scale 200 µm. C1: control group, C2: PBM group, C3: Nano-bone group, and C4: combined group of nano-bone and PBM; woven bone formation is shown after four weeks

Table 3. Results of the Scoring System Used for Bone Healing

| Group | Score | Score 0 | | Score 1 | | Score 2 | | Score 3 | | Score 4 | | P Value |
|-----------|---------|---------|--------|---------|-------|---------|-------|---------|-------|---------|-------|---------|
| | | n | % | n | % | n | % | n | % | n | % | |
| Group I | 1 week | 10 | 100.0% | 0 | 0.0% | 0 | 0.0% | 0 | 0.0% | 0 | 0.0% | <0.05 |
| | 2 weeks | 2 | 20.0% | 5 | 50.0% | 0 | 0.0% | 0 | 0.0% | 0 | 0.0% | |
| | 4 weeks | 0 | 0.0% | 3 | 30.0% | 2 | 20.0% | 2 | 20.0% | 3 | 30.0% | |
| Group II | 1 week | 10 | 100.0% | 0 | 0.0% | 0 | 0.0% | 0 | 0.0% | 0 | 0.0% | <0.001 |
| | 2 weeks | 0 | 00.0% | 7 | 70.0% | 3 | 30.0% | 0 | 0.0% | 0 | 0.0% | |
| | 4 weeks | 0 | 0.0% | 1 | 10.0% | 2 | 20.0% | 3 | 30.0% | 4 | 40.0% | |
| Group III | 1 week | 10 | 100.0% | 3 | 60.0% | 0 | 0.0% | 0 | 0.0% | 0 | 0.0% | <0.01 |
| | 2 weeks | 0 | 0.0% | 7 | 70.0% | 0 | 30.0% | 0 | 0.0% | 0 | 0.0% | |
| | 4 weeks | 0 | 0.0% | 0 | 0.0% | 2 | 20.0% | 4 | 40.0% | 4 | 40.0% | |
| Group IV | 1 week | 10 | 100.0% | 0 | 0.0% | 0 | .0% | 0 | 0.0% | 0 | 0.0% | <0.001 |
| | 2 weeks | 0 | 0% | 5 | 50% | 5 | 50.0% | 0 | 0.0% | 0 | 0.0% | |
| | 4 weeks | 0 | 00.0% | 0 | 0.0% | 0 | 0% | 0 | 0% | 10 | 100 % | |
| P value | | 0.05 | | 0.05 | | <0.001 | | <0.001 | | <0.001 | | |

Discussion

In recent decades, there has been a growing utilization of PBM and nanotechnology in the field of regenerative medicine. This advancement has the potential to impact bone biology and has become increasingly intriguing as the understanding of the connections between bone cells, laser irradiation, and nanoscale biomaterials has

grown.¹¹⁻³¹

Thus, the purpose of the present research was to evaluate and compare the impact of PBM and nano-bone on bone regeneration of mandibular bone defects in rats.

In the current study, the four-millimeter diameter bone defect created near the mandibular angle was a suitable model to determine the efficacy of different methods of

regeneration after one, two and four weeks. This was done in the same way as a previous study.²⁸

The histological results of this research showed that there was a significant variance in the mean percentage of newly formed bone between the experimental groups and the control group ($P > 0.05$). This suggests that both PBM and nano-bone have beneficial impacts on bone defect regeneration, which is according to the findings of previous research.¹²⁻¹⁸ The study showed that the greatest proportion of freshly generated bone was correlated with the use of nano-bone and PBM. This research provides evidence for the effectiveness of PBM and nano-bone in promoting bone formation throughout the healing of bone defects. This effect may be attributed to their ability to distinguish undifferentiated mesenchymal cells into osteoblasts,¹¹⁻¹³ promote osteosynthesis, reduce osteoclastic activity, and exhibit anti-inflammatory properties.¹⁻²

The histological findings of the present study suggested that group IV had the best results in terms of the amount of bone formed and inflammatory response when compared with group II, group III and the control group at all evaluation periods. By the end of 4 weeks, bone maturation with thicker and well-organized (lamellated) trabecula was obvious with a statistically significant variation ($P < 0.05$). Some researchers found similar results.¹⁴⁻¹⁸ The consistency between the findings of these research studies and the current one may be attributable to the synergistic impact of the combined utilization of PBM and nano-bone.

The percentage of newly formed bone in the two experimental groups (PBM and nano-bone) was nearly the same without a noticeable statistically difference after 4 weeks ($P > 0.05$). This may be attributed to the stimulatory impacts of PBM on the proliferation and differentiation of osteoblasts as it stimulates the differentiation of preosteoblasts to osteoblasts, reduces inflammation, and stimulates angiogenesis. This is in accordance with several studies.⁸⁻¹³ In addition, nano-bone increases new bone regeneration by promoting angiogenesis and stimulates the proliferation of osteoblasts at the bone defect.²⁰⁻²² These results agree with many recent studies that evaluated the efficacy of nano-bone in the treatment of bone defects.^{23,24}

In the current study, histological examination of group III showed bone formation represented by osteoid tissue and new bone formation were seen within the bone defect after 2 weeks. By the end of 4 weeks, well-developed lamellar bone trabeculae with a basophilic reversal line were observed. The histological analysis conducted in this study demonstrated statistically significant distinctions in favor of group III compared to group I (control) at all evaluation intervals. The elevated surface area, surface roughness, and wettability of nano-bone may contribute to several favorable biological impacts. These benefits

include higher protein adsorption and higher adhesion, differentiation, and proliferation of osteoblasts and MSCs. The findings were validated by de Almeida et al,³² who demonstrated that nano-bone had a higher amount of remaining biomaterial compared to control groups ($P = 0.007$). Additionally, there was a notable distinction in the levels of newly generated bone and connective tissue between the nano-bone group and the control groups after 42 days. The research determined that the use of nano-bone resulted in enhanced healing of the alveolar bone during a period of seven to forty-two days after operation. This enhances the positive impact of nano-bone on the process of bone repair.

In this study, marked vascularity and fibroblastic activity were observed in group II at one-week and two-week evaluation periods. This may be correlated to the stimulatory effect of vascular endothelial growth factor, which is a key player in angiogenesis by PBM. These results may be explained by a previous in-vitro study by Abdelgawad et al.⁷ On the cell line of odontoblasts, it was found that cells treated with PBM showed increased gene expression of vascular endothelial growth factor which stimulated angiogenesis. Moreover, another study by Abdelgawad et al⁵ on the cell line of osteoblast collected on day 21 reached peak mineralization which was significantly greater than that of the control group. The researchers determined that PBM was superior to the control group in terms of alkaline phosphatase expression and mineralization induction. The much higher expression of RUNX and osteocalcin supports this conclusion, which is in line with the findings of the present research.

Limitations of the Current Research

The limitations of the present study include the small numbers of animals in each group and the reporting of only short-term results (1, 2 and 4 weeks). To further confirm the effects of PBM and nano-bone on bone regeneration, researchers should include a larger number of animals and a long-term follow-up in future studies.

In the future, the current model can be enhanced by additional design of other groups with different nano-materials or different bone regenerative materials with laser PBM with different types of lasers, for studying different combinations of treatment. In this way, the most effective treatment protocol for bone regeneration can be determined.

Conclusion

Within the limits of the present research, the use of PBM by 100 mw of a 980 nm diode laser for one minute for three sessions in combination with nano-bone promoted bone regeneration. Further studies are required to support the beneficial biomodulatory effect of PBM with nano-bone as a new treatment strategy for more efficient management

of bone defects in oral and maxillofacial surgeries.

Authors' Contribution

Conceptualization: Latifa Mohamed Abdelgawad, Kawashty Ali Mohamed, Ahmed Abbas Zaky.

Data curation: Latifa Mohamed Abdelgawad.

Formal analysis: Latifa Mohamed Abdelgawad.

Methodology: Latifa Mohamed Abdelgawad, Kawashty Ali Mohamed.

Resources: Latifa Mohamed Abdelgawad, Kawashty Ali Mohamed.

Software: Kawashty Ali Mohamed, Ahmed Abbas Zaky.

Supervision: Latifa Mohamed Abdelgawad, Ahmed Abbas Zaky.

Validation: Latifa Mohamed Abdelgawad, Kawashty Ali Mohamed.

Visualization: Latifa Mohamed Abdelgawad, Kawashty Ali Mohamed.

Writing—original draft: Latifa Mohamed Abdelgawad, Kawashty Ali Mohamed.

Writing—review & editing: Latifa Mohamed Abdelgawad.

Competing Interests

None declared.

Ethical Approval

The institutional Animal Care and Use Committee (IACUC) at Cairo University, Egypt, granted approval for this animal investigation (Protocol No: CU/IF/21/21). All the procedures were conducted in accordance with international and institutional animal care, Cairo University, following the regulations and guidelines. Every effort was made to decrease the number of animals utilized and to minimize animal suffering.

Funding

None.

References

1. Le JM, Wu JH, Jaw FS, Su CT. The effect of bone remodeling with photobiomodulation in dentistry: a review study. *Lasers Med Sci.* 2023;38(1):265. doi: [10.1007/s10103-023-03933-9](https://doi.org/10.1007/s10103-023-03933-9).
2. Sleep SL, Skelly D, Love RM, George R. Bioenergetics of photobiomodulated osteoblast mitochondrial cells derived from human pulp stem cells: systematic review. *Lasers Med Sci.* 2022;37(3):1843-53. doi: [10.1007/s10103-021-03439-2](https://doi.org/10.1007/s10103-021-03439-2).
3. Qiao K, Xu L, Tang J, Wang Q, Lim KS, Hooper G, et al. The advances in nanomedicine for bone and cartilage repair. *J Nanobiotechnology.* 2022;20(1):141. doi: [10.1186/s12951-022-01342-8](https://doi.org/10.1186/s12951-022-01342-8).
4. Gulati K, Abdal-Hay A, Ivanovski S. Novel nano-engineered biomaterials for bone tissue engineering. *Nanomaterials (Basel).* 2022;12(3):333. doi: [10.3390/nano12030333](https://doi.org/10.3390/nano12030333).
5. Abdelgawad LM, Abdelaziz AM, Sabry D, Abdelgwad M. Influence of photobiomodulation and vitamin D on osteoblastic differentiation of human periodontal ligament stem cells and bone-like tissue formation through enzymatic activity and gene expression. *Biomol Concepts.* 2020;11(1):172-81. doi: [10.1515/bmc-2020-0016](https://doi.org/10.1515/bmc-2020-0016).
6. Moheghi A, Noori Moughesi SM, Amini A, Mostafavinia A, Rezaei F, Bagheri Tadi F, et al. Anti-inflammatory, antioxidant, and wound-healing effects of photobiomodulation on type-2 diabetic rats. *J Lasers Med Sci.* 2023;14:e45. doi: [10.34172/jlms.2023.45](https://doi.org/10.34172/jlms.2023.45).
7. Abdelgawad LM, Salah N, Sabry D, Abdelgwad M. Efficacy of photobiomodulation and vitamin D on odontogenic activity of human dental pulp stem cells. *J Lasers Med Sci.* 2021;12:e30. doi: [10.34172/jlms.2021.30](https://doi.org/10.34172/jlms.2021.30).
8. Tsuka Y, Kunimatsu R, Gunji H, Sakata S, Nakatani A, Oshima S, et al. Effect of Er:YAG laser irradiation on bone metabolism-related factors using cultured human osteoblasts. *J Lasers Med Sci.* 2023;14:e9. doi: [10.34172/jlms.2023.09](https://doi.org/10.34172/jlms.2023.09).
9. Surendranath P, Arjunker R. Low-level laser therapy—a review. *IOSR J Dent Med Sci.* 2013;12(5):56-9.
10. Rando RG, Buchaim DV, Cola PC, Buchaim RL. Effects of photobiomodulation using low-level laser therapy on alveolar bone repair. *Photonics.* 2023;10(7):734. doi: [10.3390/photonics10070734](https://doi.org/10.3390/photonics10070734).
11. Berni M, Brancato AM, Torriani C, Bina V, Annunziata S, Cornella E, et al. The role of low-level laser therapy in bone healing: systematic review. *Int J Mol Sci.* 2023;24(8):7094. doi: [10.3390/ijms24087094](https://doi.org/10.3390/ijms24087094).
12. Hanna R, Dalvi S, Amaroli A, De Angelis N, Benedicenti S. Effects of photobiomodulation on bone defects grafted with bone substitutes: a systematic review of in vivo animal studies. *J Biophotonics.* 2021;14(1):e202000267. doi: [10.1002/jbio.202000267](https://doi.org/10.1002/jbio.202000267).
13. Escudero JS, Perez MG, de Oliveira Rosso MP, Buchaim DV, Pomini KT, Guissoni Campos LM, et al. Photobiomodulation therapy (PBMT) in bone repair: a systematic review. *Injury.* 2019;50(11):1853-67. doi: [10.1016/j.injury.2019.09.031](https://doi.org/10.1016/j.injury.2019.09.031).
14. Doğan GE, Demir T, Orbak R. Effect of low-level laser on guided tissue regeneration performed with equine bone and membrane in the treatment of intrabony defects: a clinical study. *Photomed Laser Surg.* 2014;32(4):226-31. doi: [10.1089/pho.2013.3664](https://doi.org/10.1089/pho.2013.3664).
15. de Almeida AL, Medeiros IL, Cunha MJ, Sbrana MC, de Oliveira PG, Esper LA. The effect of low-level laser on bone healing in critical size defects treated with or without autogenous bone graft: an experimental study in rat calvaria. *Clin Oral Implants Res.* 2014;25(10):1131-6. doi: [10.1111/clr.12239](https://doi.org/10.1111/clr.12239).
16. Rasouli Ghahroudi AA, Rokn AR, Kalhori K, Khorsand A, Pournabi A, Pinheiro AL, et al. Effect of low-level laser therapy irradiation and Bio-Oss graft material on the osteogenesis process in rabbit calvarium defects: a double-blind experimental study. *Lasers Med Sci.* 2014;29(3):925-32. doi: [10.1007/s10103-013-1403-5](https://doi.org/10.1007/s10103-013-1403-5).
17. Jahangirnezhad M, Amiri M, Asareh F. Histologic examination of the effects of low-level diode laser irradiation and nano-hydroxyapatite grafting materials on ossification process on rat calvaria defects. *Int J Adv Biotechnol Res.* 2017;8(4):1121-8.
18. Pinheiro AL, de Assis Limeira Júnior F, Gerbi ME, Ramalho LM, Marzola C, Ponzi EA. Effect of low-level laser therapy on the repair of bone defects grafted with inorganic bovine bone. *Braz Dent J.* 2003;14(3):177-81. doi: [10.1590/s0103-64402003000300007](https://doi.org/10.1590/s0103-64402003000300007).
19. Huang H, Feng W, Chen Y, Shi J. Inorganic nanoparticles in clinical trials and translations. *Nano Today.* 2020;35:100972. doi: [10.1016/j.nantod.2020.100972](https://doi.org/10.1016/j.nantod.2020.100972).
20. Chandrakala V, Aruna V, Angajala G. Review on metal nanoparticles as nanocarriers: current challenges and perspectives in drug delivery systems. *Emergent Mater.* 2022;5(6):1593-615. doi: [10.1007/s42247-021-00335-x](https://doi.org/10.1007/s42247-021-00335-x).
21. Bharadwaz A, Jayasuriya AC. Recent trends in the application of widely used natural and synthetic polymer nanocomposites in bone tissue regeneration. *Mater Sci Eng C Mater Biol Appl.* 2020;110:110698. doi: [10.1016/j.msec.2020.110698](https://doi.org/10.1016/j.msec.2020.110698).
22. Hakam HM, Abdel Moneim RA, El Deeb MF. Osteoinductive potential and bone healing capacity of nanocrystalline hydroxyapatite (nHA) versus bio-dentine of surgically

- created defects in rabbits' alveolar process (an animal study). *Egypt J Histol.* 2020;43(3):902-17. doi: [10.21608/ejh.2019.16561.1164](https://doi.org/10.21608/ejh.2019.16561.1164).
23. Liu Y, Xu Z, Qiao M, Cai H, Zhu Z. Metal-based nano-delivery platform for treating bone disease and regeneration. *Front Chem.* 2022;10:955993. doi: [10.3389/fchem.2022.955993](https://doi.org/10.3389/fchem.2022.955993).
24. Gotz W, Papageorgiou SN. Molecular, cellular and pharmaceutical aspects of synthetic hydroxyapatite bone substitutes for oral and maxillofacial grafting. *Curr Pharm Biotechnol.* 2017;18(1):95-106. doi: [10.2174/1389201017666161202103218](https://doi.org/10.2174/1389201017666161202103218).
25. Wang Q, Yan J, Yang J, Li B. Nanomaterials promise better bone repair. *Mater Today.* 2016;19(8):451-63. doi: [10.1016/j.mattod.2015.12.003](https://doi.org/10.1016/j.mattod.2015.12.003).
26. Pilloni A, Pompa G, Saccucci M, Di Carlo G, Rimondini L, Brama M, et al. Analysis of human alveolar osteoblast behavior on a nano-hydroxyapatite substrate: an in vitro study. *BMC Oral Health.* 2014;14:22. doi: [10.1186/1472-6831-14-22](https://doi.org/10.1186/1472-6831-14-22).
27. Hanafiah OA, Hanafiah DS, Dohude GA, Satria D, Livita L, Moudy NS, et al. Effects of 3% binahong (*Anredera cordifolia*) leaf extract gel on alveolar bone healing in post-extraction tooth socket wound in Wistar rats (*Rattus norvegicus*). *F1000Res.* 2021;10:923. doi: [10.12688/f1000research.72982.2](https://doi.org/10.12688/f1000research.72982.2).
28. Higeuchi M, Namaki S, Furukawa A, Yonehara Y. Radiological and histochemical study of bone regeneration using the costal cartilage in rats. *J Oral Sci.* 2023;65(2):90-5. doi: [10.2334/josnusd.22-0447](https://doi.org/10.2334/josnusd.22-0447).
29. Feldman AT, Wolfe D. Tissue processing and hematoxylin and eosin staining. *Methods Mol Biol.* 2014;1180:31-43. doi: [10.1007/978-1-4939-1050-2_3](https://doi.org/10.1007/978-1-4939-1050-2_3).
30. Li J, Sheng Z, Sun J, Wang R, Yu X. Characterizations of alveolar repair after mandibular second molar extraction: an experimental study in rats. *J Appl Oral Sci.* 2022;30:e20220010. doi: [10.1590/1678-7757-2022-0010](https://doi.org/10.1590/1678-7757-2022-0010).
31. Son JH, Park BS, Kim IR, Sung IY, Cho YC, Kim JS, et al. A novel combination treatment to stimulate bone healing and regeneration under hypoxic conditions: photobiomodulation and melatonin. *Lasers Med Sci.* 2017;32(3):533-41. doi: [10.1007/s10103-017-2145-6](https://doi.org/10.1007/s10103-017-2145-6).
32. de Almeida CD, Sartoretto SC, Alves A, de Brito Resende RF, de Albuquerque Calasans-Maia J, Moraschini V, et al. Does melatonin associated with nanostructured calcium phosphate improve alveolar bone repair? *Medicina (Kaunas).* 2022;58(12):1720. doi: [10.3390/medicina58121720](https://doi.org/10.3390/medicina58121720).